

Structural and kinetic studies of the polymerization reactions of ϵ -caprolactone catalyzed by (pyrazol-1-ylmethyl)pyridine Cu(II) and Zn(II) complexes†

Cite this: *Dalton Trans.*, 2013, **42**, 10735

Stephen O. Ojwach,^{*a} Teddy T. Okemwa,^b Nelson W. Attandoh^a and Bernard Omondi^c

The structural and kinetic studies of polymerization reactions of ϵ -caprolactone (ϵ -CL) using (pyrazolylmethyl)pyridine Cu(II) and Zn(II) complexes as initiators is described. Reactions of 2-(3,5-dimethylpyrazol-1-ylmethyl)pyridine (**L1**) and 2-(3,5-diphenylpyrazol-1-ylmethyl)pyridine (**L2**) with Zn(Ac)₂·2H₂O or Cu(Ac)₂·2H₂O produced the corresponding complexes [Zn(Ac)₂(**L1**)] (**1**), [Cu(Ac)₂(**L1**)] (**2**), [Zn(Ac)₂(**L2**)] (**3**) and [Cu₂(Ac)₄(**L2**)₂] (**4**) respectively. Solid state structures of **1** and **4** confirmed that complexes **1** and **4** are monomeric and dimeric respectively and that **L1** is bidentate in **1** while **L2** is monodentate in **4**. X-band EPR spectra of **2** and **4** revealed that complex **2** is monomeric both in solid and solution state, while the paddle-wheel structure of **4** is retained in solution. Complexes **1–4** formed active initiators in the ring opening polymerization of ϵ -CL. Zn(II) complexes **1** and **3** exhibited higher rate constants of 0.044 h⁻¹ and 0.096 h⁻¹ respectively compared to rate constants of 0.017 h⁻¹ and 0.031 h⁻¹ observed for the corresponding Cu(II) complexes **2** and **4** respectively at 110 °C. All the polymerization reactions follow pseudo first-order kinetic with respect to ϵ -CL monomer. Initiator **1** showed first-order dependency on the polymerization reactions and utilizes only one active site as the initiating group. The molecular weights of the polymers produced range from 1982 g mol⁻¹ to 14 568 g mol⁻¹ and exhibited relatively broad molecular weight distributions associated with transesterification reactions.

Received 22nd May 2013,

Accepted 4th June 2013

DOI: 10.1039/c3dt51338f

www.rsc.org/dalton

Introduction

Polyesters derived from renewable resources have attracted considerable attention over the last decades as biocompatible and biodegradable alternatives to petrochemical-based plastics.¹ In particular, polycaprolactone (PCL) has found varied applications in biomedical and pharmaceutical fields.² These aliphatic polyesters are traditionally prepared *via* ring opening

polymerization (ROP) of cyclic esters through a coordination–insertion pathway involving a metal alkoxide catalyst.³ This route has the potential to offer stereo-selectivity and control of molecular weight of the polymers produced.⁴ Furthermore, kinetic studies provide detailed mechanistic information pertaining to this pathway⁵ including insight into effects of catalyst structure on polymerization activity.⁶

To date, the design of well-defined catalysts that could produce polyesters with desirable molecular weight and narrow molecular weight distribution still remains a daunting task. While tin-based systems⁷ show promising results in terms of control of polymer molecular weight and good activity, their toxicity limits their industrial appeal.⁸ Several discrete complexes ranging from metallocenes⁹ to early transition metal complexes like Ti,¹⁰ Zr,¹¹ Hf¹² have been investigated as catalyst initiators for the ROP of cyclic esters. Despite encouraging results in these studies, numerous challenges namely; catalyst stability, poor control of polymer microstructure to cost of the catalysts are hindering their commercialization. One group of complexes that have the propensity to produce effective catalysts for the ROP polymerization of cyclic esters are the Zn(II) and Cu(II) complexes.¹³ The suitability of these complexes emanates from their ease of synthesis,

^aSchool of Chemistry and Physics, University of KwaZulu-Natal, Pietermaritzburg Campus, Private Bag X01 Scottsville, 3209, South Africa. E-mail: ojwach@ukzn.ac.za; Fax: +27 (33) 260 5009; Tel: +27 (33) 260 5239

^bDepartment of Chemistry, Maseno University, P. O. Box 333, Maseno, 4105, Kenya

^cSchool of Chemistry and Physics, University of KwaZulu-Natal, Westville Campus, Private Bag X54001, Durban, 4000, South Africa

† Electronic supplementary information (ESI) available: Supplementary Fig. S1–S7 represent graphs of the percentage conversions of ϵ -CL to PCL for catalysts **1–4** (S1), ¹H NMR spectra for the determination of the rates of polymerization (S2), plot of ln[CL]₀/[CL]_t vs. time for **1** at different concentrations (S3), plot of ln[CL]₀/[CL]_t vs. time for **2** at different catalyst concentrations depicting the longer induction periods (S4); plot of *k*_{obs} vs. [1] for the determination of threshold catalyst concentration (S5) and GPC chromatograms for PCL obtained (S6–S8). CCDC numbers 828074 and 927444 contain the supplementary crystallographic data for **1** and **4**. For ESI and crystallographic data in CIF or other electronic format see DOI: 10.1039/c3dt51338f

stability and more significantly their biocompatibility. Recently, Zn(II) α -diimine complexes were reported to portray both control of polymer stereo-regularity and excellent activity in the ROP of lactides.¹⁴ This control of polymer microstructure is largely influenced by the steric bulk of the ligand used, and as such careful design of the ligand motif could result in controlled ROP of the cyclic esters.

In this current contribution, we explore the potential use of (pyrazol-1-ylmethyl)pyridine Zn(II) and Cu(II) acetate complexes as catalyst initiators in the ROP of ϵ -CL. We envisage that, by regulating the steric bulk on the ligand backbone, proper control of polymer molecular weight and molecular weight distribution could be achieved. Detailed structural and kinetics studies have been performed in order to elucidate the effect of catalyst structure and nature of active species on the polymerization behaviour of the complexes. These findings are herein discussed.

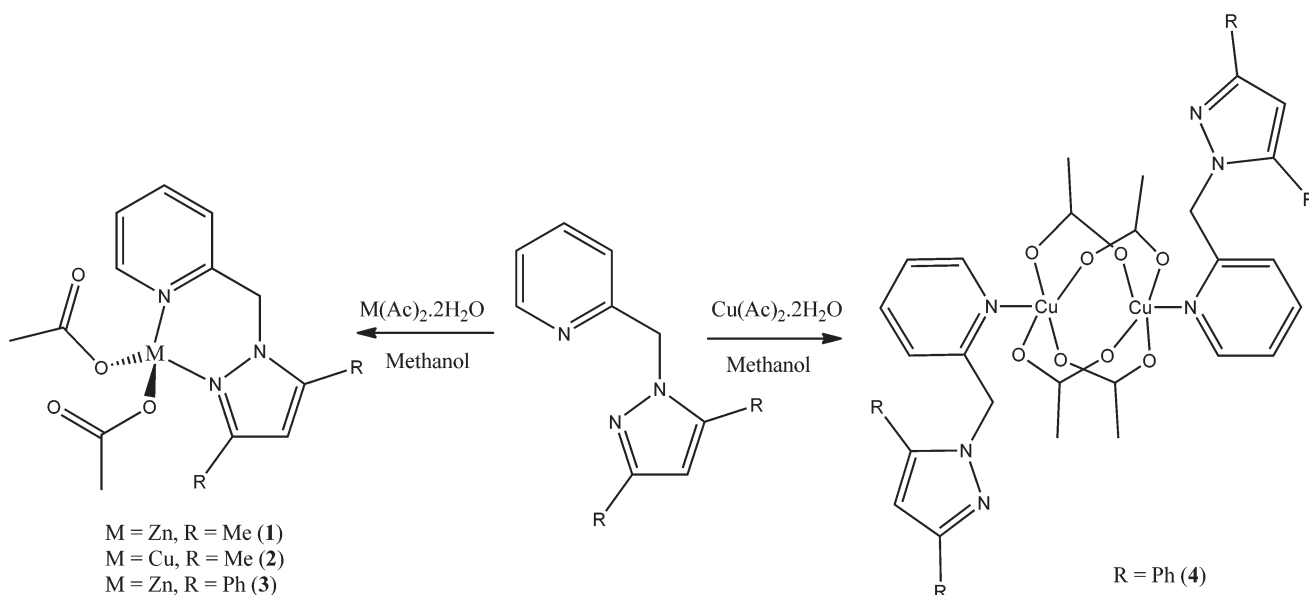
Results and discussion

Synthesis and structural characterization of Zn(II) and Cu(II) (pyrazol-1-ylmethyl)pyridine complexes 1–4

Reactions of 2-(3,5-dimethylpyrazol-1-ylmethyl)pyridine (**L1**) and 2-(3,5-diphenylpyrazol-1-ylmethyl)pyridine (**L2**) with Zn(Ac)₂·2H₂O produced the corresponding monometallic Zn(II) complexes [Zn(Ac)₂(**L1**)] (**1**) and [Zn(Ac)₂(**L2**)] (**3**). Similarly treatment of **L1** and **L2** with Cu(Ac)₂·2H₂O produced monometallic and bimetallic complexes [Cu(Ac)₂(**L1**)] (**2**) and [Cu₂(Ac)₄(**L2**)₂] (**4**) respectively (Scheme 1). Complexes **1–4** were obtained in moderate to high yields (62%–81%). Complexes **1** and **3** were isolated as pale yellow solids, while **2** and **4** were obtained as blue solids.

The compounds were characterized by ¹H NMR spectroscopy for **1** and **3**, mass spectrometry, elemental analyses and single crystal X-ray crystallography for **1** and **4**. ¹H NMR spectra of complexes **1** and **3** showed a singlet peak at about 2.10 ppm, diagnostic of the acetate protons. In addition, a singlet peak observed at 5.46 ppm and 5.59 ppm in **1** and **3** respectively were assigned to the CH₂ linker protons. Microanalyses data of **1–4** were consistent with one metal atom per ligand unit as shown in Scheme 1, and also confirmed their purity. Mass spectra of **1–4** showed *m/z* peaks corresponding to the fragments of the parent compounds. For example, the mass spectra of **1** and **2** showed base peaks at *m/z* = 310 and 309 respectively, associated with the loss of one acetate ligand [M⁺ – Ac]. The absence of the molecular ions [M⁺] could originate from the lower stability of the parent compounds under the ionization conditions.¹⁵

Single crystals suitable for X-ray crystallography analyses for **1** and **4** were grown by slow diffusion of hexane into a dichloromethane solution of the complexes. Data collection and structure refinement parameters are given in Table 1 while Fig. 1 and 2 show the molecular structures and bond parameters for **1** and **4** respectively. In the solid structure of **1**, **L1** adopts a bidentate coordination mode. The acetate as a ligand displays a wide variety of binding modes similar to carbonate and nitrate ligands: it can act as monodentate, bidentate and anisodentate. Due to this flexibility in its coordination behaviour, we have used a literature method¹⁶ to deduce the denticity of the acetate ligand in **1**. The differences between the two M–O_{nitrate} bond distances (Δd) and M–O–C bond angles ($\Delta\theta$) are used to classify the denticity ($\Delta d < 0.3$ Å and $\Delta\theta < 14^\circ$ for bidentate; 0.3 Å $< \Delta d < 0.6$ Å and $14^\circ < \Delta\theta < 28^\circ$ for anisodentate ($\Delta d > 0.6$ Å and $\Delta\theta > 28^\circ$ for monodentate). Using this approach, one acetate ligand is clearly monodentate while the other one is anisodentate ($\Delta d = 0.6$ Å and $\Delta\theta = 17^\circ$) in **1**. The



Scheme 1

Table 1 Crystal data collection and structural refinement parameters for **1** and **4**

Parameters	1	4
Empirical formula	C ₁₅ H ₁₉ N ₃ O ₄ Zn	C ₅₀ Cu ₂ H ₄₆ O ₈ N ₆ O ₈
Formula weight	370.70	986.01
Temperature	100(2) K	100(2) K
Wavelength	0.71073 Å	0.71073 Å
Crystal system	Orthorhombic	Triclinic
Space group	<i>Pna</i> 21	<i>P</i> $\bar{1}$
<i>a</i> /Å	14.7323(10)	9.6202(3)
<i>b</i> /Å	8.1094(5)	10.6016(3)
<i>c</i> /Å	13.5844(8)	11.7735(3)
α	90°	72.8800(10)°
β	90°	75.3930(10)°
γ	90°	78.1930(10)°
Volume (Å ³)	1622.93(18)	1099.39(3)
<i>Z</i>	4	1
Density (calculated)	1.517 Mg m ⁻³	1.489 Mg m ⁻³
Absorption coefficient	1.536 mm ⁻¹	1.032 mm ⁻¹
<i>F</i> (000)	768	510
Crystal size (mm ³)	0.14 × 0.14 × 0.06	0.41 × 0.27 × 0.15
Theta range for data collection	2.77 to 28.35°	1.85 to 28.52°
Index ranges	-19 ≤ <i>h</i> ≤ 19; -10 ≤ <i>k</i> ≤ 10; -17 ≤ <i>l</i> ≤ 18	-12 ≤ <i>h</i> ≤ 12; -12 ≤ <i>k</i> ≤ 14; -15 ≤ <i>l</i> ≤ 15
Reflections collected	30 990	27 490
Independent reflections	4040 [<i>R</i> (int) = 0.0474]	5516 [<i>R</i> (int) = 0.0248]
Completeness to theta	(=28.35°) 99%	(=28.52°) 98.8%
Max and min transmission	0.9135 and 0.8137	0.8606 and 0.6771
Absorption correction	Semi-empirical from equivalents	Semi-empirical from equivalents
Data/restraints/parameters	4040/4/213	5516/0/300
Goodness-of-fit on <i>F</i> ²	1.029	1.030
Final <i>R</i> indices [<i>I</i> > 2σ(<i>I</i>)]	<i>R</i> ₁ = 0.0253, <i>wR</i> ₂ = 0.0574	<i>R</i> ₁ = 0.0243, <i>wR</i> ₂ = 0.0667
<i>R</i> indices (all data)	<i>R</i> ₁ = 0.0300, <i>wR</i> ₂ = 0.0593	<i>R</i> ₁ = 0.0260, <i>wR</i> ₂ = 0.0683
Largest diff. peak and hole	0.398 and -0.182 e Å ⁻³	0.472 and -0.488 e Å ⁻³

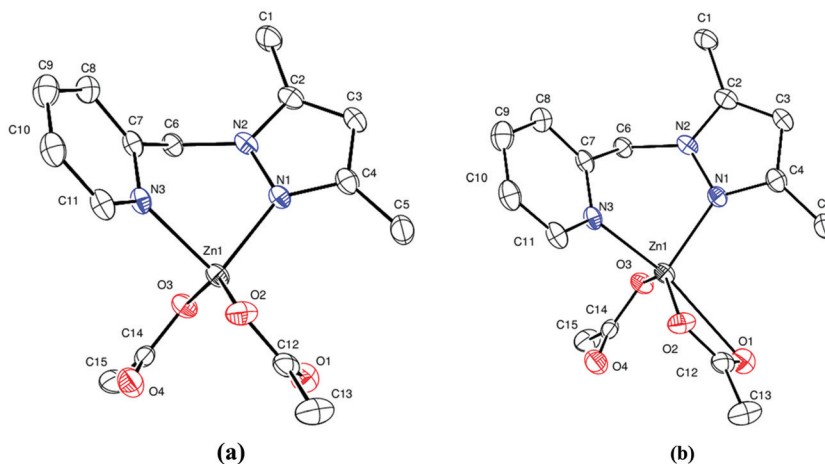


Fig. 1 Molecular structure of complex **1** showing both the four-coordinate (a) and five coordinate (b) geometries drawn with 50% probability thermal ellipsoids. Hydrogen atoms are omitted for clarity. Selected bond lengths [Å] and angles (°): O(2)–Zn(1), 1.9653(8); O(3)–Zn(1), 1.9649(13); O(1)–Zn(1), 2.566(2); Zn–N(1), 2.066(2); Zn(1)–N(3), 2.102(2). O(3)–Zn(1)–O(2), 141.14(6); O(3)–Zn(1)–N(1), 96.89(7); O(2)–Zn(1)–N(1), 115.81(7); O(3)–Zn(1)–N(3), 103.52(4); O(2)–Zn(1)–N(3), 97.21(7); N(1)–Zn(1)–N(3), 89.99(6).

geometry around the Zn atom in **1** could thus be best described as distorted tetrahedral (Fig. 1a). Five-coordination sphere to give a trigonal bipyramidal geometry is also likely in the case of bidentate coordination of the anisodentate acetate ligand (Fig. 1b). This fluxionality has the potential to influence the catalytic behaviour of **1**, where a given geometry exhibits different catalytic behaviour. The bond angles around the Zn(II) atom of between 89.99(6)° for N(1)–Zn–N(3) to 141.14(6)°

for O(3)–Zn–O(2) significantly deviate from 109° expected for a tetrahedral geometry. This could originate from steric restrictions imposed by **L1** and flexibility of the acetate ligand. The Zn(1)–N(1) and Zn(1)–N(3) bond distances of 2.066(2) Å and 2.102(2) Å respectively are normal and comparable to those of related compounds in literature.¹⁷ The average Zn–O_{acetate} bond lengths of 1.965(2) Å fall within the expected range of Zn–O_{acetate} distances.¹⁸

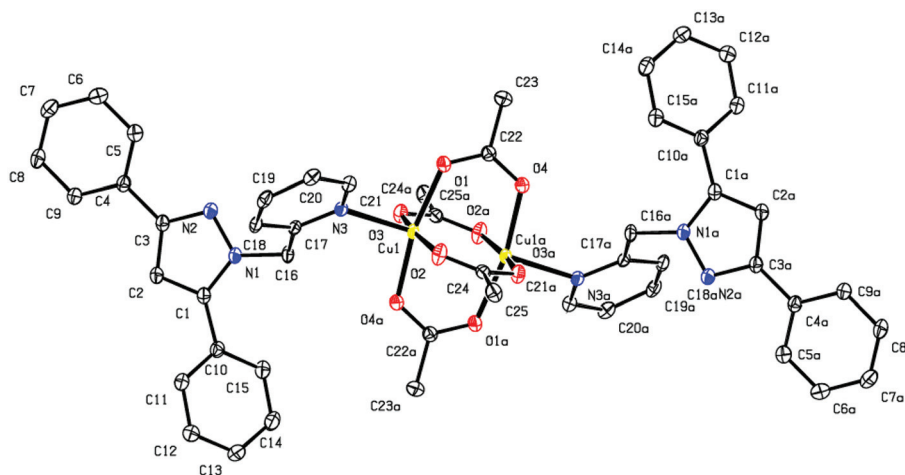


Fig. 2 Molecular structure of the paddle wheel copper complex **4** drawn with 50% probability thermal ellipsoids. Hydrogen atoms are omitted for clarity. Selected bond lengths [Å] and angles (°): O(1)–Cu(1), 1.9748(9); O(2)–Cu(1), 1.9875(9); O(3)–Cu(1), 1.9716(9); O(4)–Cu(1), 1.9665(9); Cu(1)–N(3), 2.2138(10). Cu(1)–Cu(1)#, 2.6532(3). O(3)–Cu(1)–O(4), 90.93(4); O(4)–Cu(1)–O(1), 168.06(4); O(3)–Cu(1)–O(1), 87.12(4); O(4)–Cu(1)–N(3), 98.52(4); O(1)–Cu(1)–N(3), 93.34(4); O(2)–Cu(1)–N(3), 89.85(4).

As depicted in Fig. 2, complex **4** exhibits a bimetallic paddle wheel conformation with an octahedral geometry around the Cu(II) atom. Interestingly, **L2** is monodentate, binding *via* the pyridine nitrogen atom, with the pyrazolyl nitrogen atom uncoordinated. This contrasts the coordination mode observed for **L1** in **1**. The four acetate ligands bridge the two Cu(II) centres to complete the octahedral arrangement. The molecule has a crystallographic C_2 -symmetry axis passing through C24 and C25 and bisecting the Cu–Cu bond thus rendering many of the atoms symmetry equivalent. The bond angles of $90.93(4)^\circ$ and $91.55(4)^\circ$ for O(4)–Cu(1)–O(3) and O(1)–Cu(1)–O(2) respectively in **4** are close to the expected bond angle of 90° for an octahedral geometry. This slight distortion could be due to reduced crowding around the Cu atom as a result of the monodentate nature of **L2**. A closer examination of the structure reveals that the bulk of the ligand resides away from the metal center. The average Cu–N_{pyridine} and Cu–O_{acetate} bond distances of 2.2138(10) Å and 1.9775(9) Å are comparable to those reported for the 2-amino pyridine Cu

complex¹⁹ of 2.0248 (3) Å and 1.991(4) Å respectively. The Cu–Cu bond distance of 2.5316(6) Å in **4** is slightly shorter than the average Cu–Cu bond lengths of 2.671(2) Å reported in literature.²⁰

EPR spectra of complexes **2** and **4**

In order to understand the coordination environment of the copper complexes both in solid state and in solution, X-band EPR spectra of **2** and **4** were acquired in solid and methanol solution at room temperature (Fig. 3). Both the solid and solution state EPR spectra of **2** (Fig. 3a) exhibited an axial (tetragonal) g -tensor with a $d_{x^2-y^2}$ ground-state doublet consistent with monomeric Cu(II) complex.^{21a} In solution state, the g_z signal of **2** shows evidence of hyperfine coupling of the single electron to the Cu(II) nucleus while in the solid state, the spectra does not exhibit copper hyperfine structure. This could be attributed to very short spin-lattice relaxation times in the solid state. Similar broad EPR spectra have been observed for some copper carboxylate dimers.^{21c,d} EPR spectra of **4** both

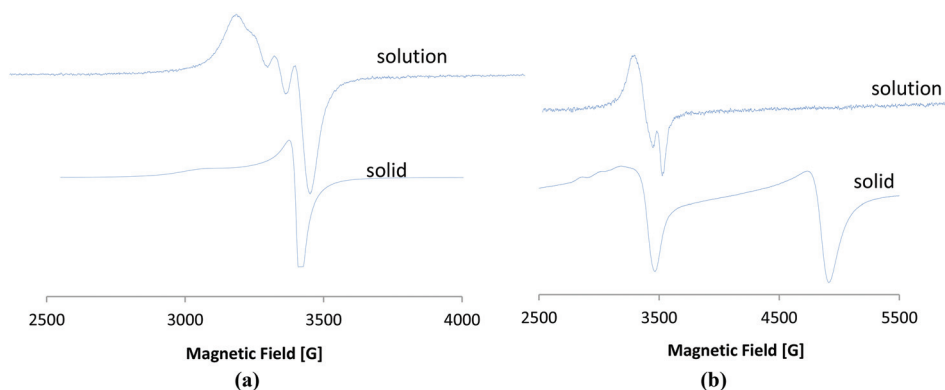


Fig. 3 X-band EPR spectra of (a) complex **2** and (b) complex **4** in solid and methanol solution at 298 K. **2** in solid: $g_z = 2.292$; $g_y = 2.069$; **2** in solution: $g_z = 2.174$; $g_y = 2.087$, $A = 61$. **4** in solution: $g_z = 2.207$; $g_y = 2.151$, $g_x = 2.0883$. **4** in solid state: $g_z = 2.211$; $g_y = 2.009$, $g_x = 1.45$.

in solid and in methanol solution (Fig. 3b) display rhombic tensor with the unpaired electron occupying the $d_{x^2-y^2}$ orbital typical of dimeric paddle-wheel structure.²² This confirms that the dimeric structure of **4** is retained in solution, consistent with stronger Cu–O bonds of carboxylates as opposed to weaker Cu–Cl bridging bonds which results in dissociations of Cu dimers when Cl is the bridging ligand.²³ The solid state EPR spectra of **4** shows evidence of hyperfine electron–Cu nucleus coupling, while no hyperfine coupling is evident in the solution spectra.^{21b,22} Smaller zero-field splitting ($A = 61$) in addition to lower g values of **2** and **4** are in good agreement with the existence of a pyridine nitrogen donor atom in the copper coordination sphere.²³ More significantly, solid state EPR spectrum of **4** demonstrates that the two Cu atoms in the dimer are not anti-ferromagnetically coupled (magnetically dilute). The longer Cu–Cu bond distance of 2.5316(6) Å in **4** compared to a Cu–Cu bond length of 2.19 Å required to achieve effective Cu–Cu metal interaction supports the EPR data.²⁴ The monomeric nature of **2** could be assigned to the less steric requirements by **L1** as opposed to the sterically demanding **L2** in **4**. From this approach, we cannot rule out the possibility of complex **3** existing as a dimer in the solid state. So far attempts to obtain single crystals suitable for X-ray analyses to confirm the solid state structures of **2** and **3** have been unsuccessful.

Polymerization of ϵ -caprolactone using 1–4 as initiators

Preliminary investigations of complexes **1–4** as catalyst initiators in the ring opening polymerization (ROP) reactions of ϵ -CL were performed at 110 °C in bulk using $[M]/[I]$ ratio of 100:1. Under these conditions, all the complexes exhibited significant catalytic activities within 24 h for **1** and **3** and 48 h for **2** and **4** (Fig. S1†). Having established that complexes **1–4** form effective initiators in the ROP of ϵ -CL, detailed mechanistic and kinetics studies were performed in order to gain insight into the nature of the active species, kinetics of the reactions and influence of catalyst structure and reaction conditions on catalyst activity and polymer properties.

Kinetics of ϵ -CL polymerization reactions

Kinetics of the ϵ -CL polymerization was investigated for complexes **1–4** by monitoring the reactions using ^1H NMR spectroscopy. Sampling was done at regular intervals and percentage conversions of ϵ -CL to PCL determined by comparing the intensity of the PCL signals at 4.0 ppm to that of the ϵ -CL monomer at 4.2 ppm (Fig. S2†). A summary of the polymerization data is given in Table 2. A plot of $\ln[\text{CL}]_0/[\text{CL}]_t$ versus time gave a linear relationship consistent with a pseudo-first order kinetics with respect to ϵ -CL for all the complexes (Fig. 4). The kinetics of the ϵ -CL polymerization reactions thus proceeded according to the simple pseudo first-order kinetics with the respect to ϵ -CL as shown in eqn (1).

$$\frac{d[\text{CL}]}{dt} = k[\text{CL}] \quad (1)$$

Table 2 Summary of ϵ -CL polymerization data by complexes **1–4**^a

Catalyst	Time (h)	Conversion (%)	Mw ^b	PDI ^b	IE ^c
1	24	43	1982	2.60	0.40
	32	68	2413	2.58	0.31
	48	94	2928	3.23	0.27
3	4	33	2121	3.13	0.56
	8	48	2454	3.24	0.45
	12	59	2845	3.48	0.42
	24	92	3853	3.33	0.37
	36	98	4111	3.74	0.37
	48	99	4726	3.92	0.42
4	48	78	2749	2.84	0.31
	72	93	3814	3.52	0.36
	96	94	4652	3.96	0.43
1 ^d	48	32	2274	3.12	0.63
	72	82	3413	3.17	0.37
3 ^d	12	45	3089	3.82	0.61
	24	73	3338	3.14	0.40
	48	98	4365	3.27	0.39

^a Reaction conditions, $[\text{CL}]_0$, 0.01 mol, temperature, 110 °C, bulk polymerization. ^b Molecular-weight average and polydispersity index (PDI) determined by GPC relative to polystyrene standards. ^c Initiator efficiency (IE) = $Mw_{\text{exp}}/Mw_{\text{calc}}$ where $Mw_{\text{calc}} = Mw_{(\text{monomer})} \times [\text{CL}]_0/[I] \times [\text{PCL}]/[\text{CL}]_0 + Mw_{(\text{chain-end groups})}$. ^d Addition of second equivalent of ϵ -CL without adding the initiator.

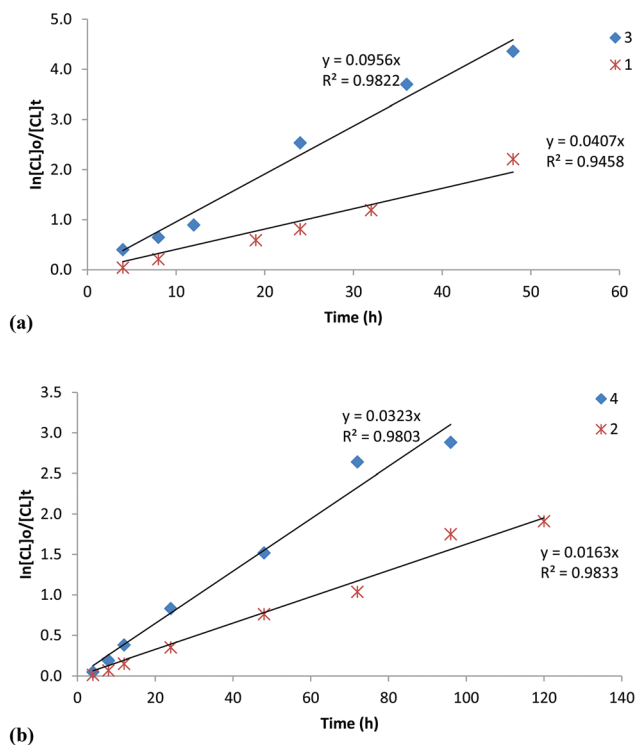


Fig. 4 First order kinetic plots of $\ln[\text{CL}]_0/[\text{CL}]_t$ vs. time for (a) Zn complexes **1** and **3** and (b) Cu complexes **2** and **4** in the bulk polymerization of ϵ -CL at 110 °C, $[\text{CL}]_0$, 0.01 mol, $[\text{CL}]_0/[I] = 100$.

where $k = k_p[I]^x$, k_p = rate of chain propagation and I = initiator; x = order of reaction.

The rate constants for initiators 1–4 were extracted from Fig. 4 and obtained as 0.044 h^{-1} (1), 0.017 h^{-1} (2), 0.096 h^{-1} (3) and 0.031 h^{-1} (4). Initiator 3 was thus the most active while initiator 2 was the least active. Higher activities observed for Zn initiators 1 and 3 in comparison to the Cu analogues 2 and 4 is consistent with literature reports.²⁵ More evident was the increase in catalytic activity with increase in steric bulk of the pyrazolyl ligand in 1–4. For instance, replacing the Me groups in 1 with the bulkier Ph groups in 3 resulted in a two-fold increase in the rate of reaction from 0.044 h^{-1} to 0.096 h^{-1} respectively. This observation agrees with the reports of Silvernail *et al.*²⁶ In our case, the bimetallic nature of 4 could be responsible for its higher activity compared to the monometallic complex 2. As argued from EPR data, it is also possible that complex 3 is bimetallic hence its greater catalytic activity than the corresponding Zn complex 1.

Comparatively, the rate constants in the polymerization of ϵ -CL for 1–4 are lower than some of the most active initiators reported.²⁷ A number of very active zinc catalysts are multinuclear and contain alkoxides as the initiating groups. For example, the trinuclear Zn complex reported by Chen *et al.* exhibits a rate constant of 0.0508 s^{-1} in the polymerization of ϵ -CL.^{27b} Despite the relative low activities of 1–4, they were found to be more active than the aluminium alkoxide catalyst reported by Zhong *et al.*²⁸ which displays apparent rate constant of 0.067 day^{-1} .

Further kinetics was performed to assess the order of the reaction with respect to initiators 1 and 3 and the overall rates of reactions. This was done by carrying out the polymerization reactions at different catalyst concentrations (Fig. S3†) at constant concentration of ϵ -CL (Table 3). A plot of $\ln[k_{\text{obs}}]$ versus $\ln[1]$ gave a linear relationship consistent with a first-order dependency of reaction on 1 (Fig. 5). The order of the reaction with respect to 1 was thus extracted from the plot of $\ln[k_{\text{obs}}]$ versus $\ln[1]$ and obtained as 0.8. Fractional orders of reaction with respect to the initiator has been previously observed²⁹ and is believed to be due to complicated

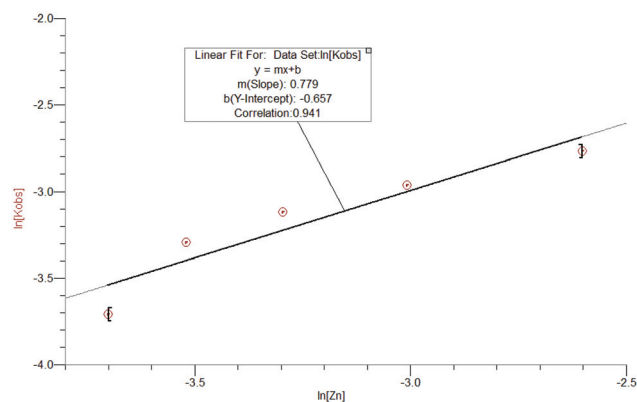


Fig. 5 Linear plots of $\ln[k_{\text{obs}}]$ vs. $\ln[1]$ polymerization of caprolactone at $[\text{CL}]_0 = 0.01 \text{ mol}$, $110 \text{ }^\circ\text{C}$ for the determination of order of reaction with respect to 1.

aggregation of the active sites during polymerization reactions.²⁹ Thus the overall rate law for ϵ -CL polymerization by 1 can be represented as shown in eqn (2). This rate law is consistent with a mechanism involving a coordinative insertion at a single Zn site. It is therefore apparent that only one Zn–O_{acetate} in complex 1 (Fig. 1) acts as the initiating group. A closer examination of $\ln[k_{\text{obs}}]$ versus $\ln[2]$ showed the presence of an induction period especially at low catalyst concentrations (Fig. S4†). This behaviour has been largely attributed to rearrangement of the coordinative aggregates in the initiator.^{30,31} For 2, this may be associated with dissociation of the Cu–Cu and Cu–O_{Ac} bonds prior to ϵ -CL coordination. Thus attempts to determine the order of the reaction with respect to initiator 2 were unsuccessful due to the longer induction periods which rendered the plots non-linear (Fig. S4†).

$$\frac{d[\text{CL}]}{dt} = k[\text{CL}][1]^{0.8} \quad (2)$$

The number of active centers (n)

To determine the number of active sites in initiator 1, a plot of the degree of polymerization (X_n) vs. $[\text{CL}]_0/[1]$ at fixed conversion was constructed (Fig. 6). Due to the linearity of the plot, the average number of the initiating sites in 1 was determined from the slope of the curve (0.788).³² Thus 1 has on average

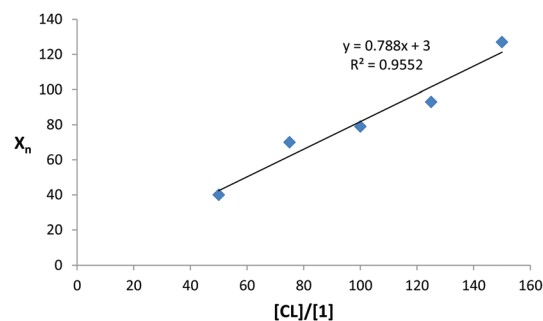


Fig. 6 Plot of degree of polymerization (X_n) of CL vs. $[\text{CL}]_0/[1]$ at fixed conversion for the determination of number of active sites in 1. The inverse of the slope 0.788 gives an average of 1.3 active sites.

Table 3 Effect of catalyst concentration, temperature and solvent on polymerization kinetics of ϵ -CL using catalyst 1^a

Entry	$[\text{CL}]_0/[1]$	Conversion ^b (%)	K_{obs} (h^{-1})	Mw ^c	PDI ^c	IE ^d
1	50	90	0.063	4610	2.82	0.90
2	75	85	0.052	8008	2.96	1.10
3	125	92	0.037	10 696	3.23	0.81
4	150	94	0.010	14 568	3.25	0.91
5	50 ^e	99	0.189	2407	2.00	0.43
6	50 ^f	99	0.026	4193	2.42	0.74
7	50 ^g	80	0.022	3119	2.52	0.68

^a Reaction conditions, $[\text{CL}]_0$, 0.01 mol, temperature, $110 \text{ }^\circ\text{C}$, bulk polymerization. ^b Maximum conversions achieved. ^c Molecular-weight average and polydispersity index (PDI) determined by GPC relative to polystyrene standards. ^d Initiator efficiency (IE) = $Mw_{\text{exp}}/Mw_{\text{calc}}$ where $Mw_{\text{calc}} = Mw_{\text{(monomer)}} \times [\text{CL}]_0/[1] \times [\text{PCL}]/[\text{CL}]_0 + Mw_{\text{(chain-end groups)}}$. ^e Solvent, methanol. ^f Solvent, toluene. ^g Temperature, $90 \text{ }^\circ\text{C}$.

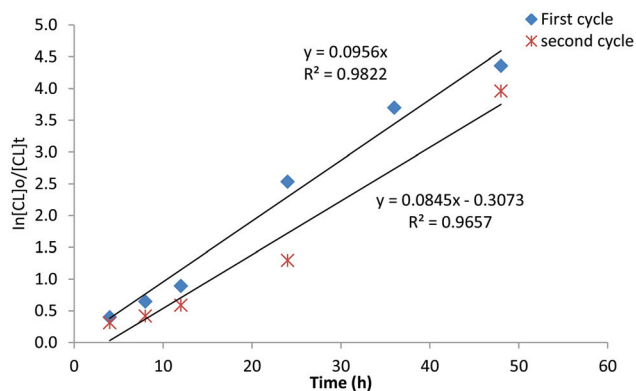


Fig. 7 First order kinetic plots of $\ln([\text{CL}]_0/[\text{CL}]_t)$ vs. time of the first and second cycle experiments for **3**, at 110 °C, $[\text{CL}]_0$, 0.01 mol, $[\text{CL}]_0/[\text{I}] = 100$. Equivalent amount of ϵ -CL monomer was added in the second cycle without adding the catalyst.

1.3 (out of a possible two) active initiating sites per complex. This data is in good agreement with the first-order dependency of the polymerization kinetics on **1** (Fig. 5). The findings that **1** does not utilize both the possible active sites (two $\text{M}-\text{O}_{\text{acetate}}$ bonds) is in agreement with several literature reports.^{32b,c}

Stability of the initiators

To provide insight into the stability of these systems, a sequential two-stage polymerization of ϵ -CL was performed using **1** and **3** (Table 2, Fig. 7). Thus the first cycle ($[\text{CL}]_0/[\text{I}] = 100$) was allowed to proceed to completion (99%) and another 100 equivalent of ϵ -CL was added without adding the initiator ($[\text{CL}]_0/[\text{I}] = 200$). For **3**, rate constants of 0.096 h^{-1} and 0.085 h^{-1} were reported in the first and second cycles respectively (Fig. 7). This translates to 12% drop in the catalytic activity of **3** in the second cycles and therefore confirms its relative stability.

Effect of temperature and solvent on ϵ -CL polymerization kinetics

The effect of temperature on the polymerization kinetics of ϵ -CL by **1** was probed by comparing the activities at 60 °C, 90 °C and 110 °C at $[\text{CL}]_0/[\text{I}]$ of 50 (Table 3). At 60 °C, **1** showed very low activity managing a paltry 25% conversion after 48 h. In addition, the reactions were characterized by longer induction periods leading to non-linear plots, hence the rate constant at 60 °C could not be evaluated. At 90 °C, the rate constant was obtained as 0.022 h^{-1} , three times lower than 0.063 h^{-1} recorded at 110 °C. It is therefore apparent that **1-4** are only active at elevated temperatures. To understand the influence of solvent on the polymerization reactions, we compared the activities of **1** in bulk, methanol and toluene solvents. The k_{obs} of 0.063 h^{-1} in the bulk polymerization was lower than 0.186 h^{-1} recorded in methanol solvent. This is consistent with the formation of a metal-alkoxide ($\text{M}-\text{OEt}$), which is known to give active initiating groups.^{27b} On the hand, use of the non-coordinating toluene solvent resulted in a drop in k_{obs} to 0.026 h^{-1} . At this stage, it is unclear why reactions in toluene resulted in decreased activity. One hypothesis is that

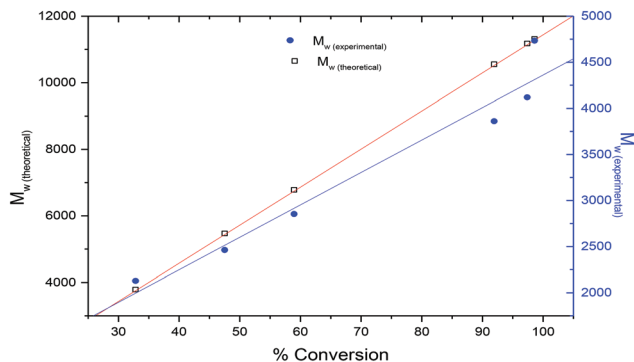


Fig. 8 Plot of experimental and calculated M_w of PCL vs. % conversion for the bulk polymerization of ϵ -CL by **3**. $[\text{CL}]_0 = 0.01$ mol, 110 °C, $[\text{3}] = 0.0001$ mol. The empty rectangles show the theoretical M_w calculated from ^1H NMR spectra while the block rectangles show the experimental M_w determined by SEC.

the use of toluene may reduce the concentrations of the reactants hence lower rates of collisions of the molecules as compared to the bulk reactions.

Molecular weight and molecular weight distribution of polycaprolactone (PCL)

The molecular weight and molecular weight distribution of the polymers were determined by GPC and compared to the theoretical values obtained from ^1H NMR calculations (Tables 2 and 3). Generally, low to moderate molecular weight polymers between 1982 g mol^{-1} to 14 568 g mol^{-1} were obtained. Consistent with living polymerization behaviour, molecular weights increased with percentage conversion (Fig. 8). For instance, molecular weights of 2121 g mol^{-1} and 4726 g mol^{-1} were obtained at 33% and 99% conversions respectively for **1**. The living polymerization nature of **1** was further augmented by the observed increase in molecular weights with increase in $[\text{CL}]_0/[\text{I}]$. For example, an increase in the $[\text{CL}]_0/[\text{I}]$ from 50 to 125 resulted in a concomitant increase in molecular weight from 4610 g mol^{-1} to 10 696 g mol^{-1} respectively (Table 3, entries 1–3). The highest initiator efficiency of 1.1 (110%) was obtained at $[\text{CL}]_0/[\text{I}]$ of 125. Despite the linear dependency of molecular weight on ϵ -CL conversion, the experimental molecular weights were significantly lower than the theoretically calculated values (Fig. 8). This was more evident at higher conversions where lower initiator efficiencies of 0.42 (42%) were reported. For example, at 95% conversion, the experimental molecular weight of 4726 g mol^{-1} was obtained, compared to the theoretical value of 11, 294 g mol^{-1} . In addition, the polymers exhibited relatively wide molecular weight distributions (2.00–3.48).

The low initiator efficiencies of **1-4** were further confirmed by the two-stage polymerization reactions. As shown in Table 2, addition of the monomer after completion of the first run resulted in a significant drop of molecular weight from 4726 g mol^{-1} (99%) to 3089 g mol^{-1} (45%); a clear indication of growth of a new polymer chain. Indeed the maximum molecular weight of 4365 g mol^{-1} obtained in the second run is lower than 4726 g mol^{-1} reported in the first. This is in

contrast to the expected behaviour of living polymerization catalysts.²⁶ For example, Silvernail *et al.* recorded an increase in molecular weight of PCL from 4200 g mol⁻¹ (run 1) to 10 400 g mol⁻¹ (run 2).²⁶ These observations point to lack of controlled ϵ -CL polymerization by 1–4. A number of factors could be responsible. One, the use of acetate ligand as the initiating group has been reported to give low molecular weight and broad PDI in comparison to the alkoxide initiators.³³ Indeed polymers obtained in methanol solvent exhibited relatively narrow PDI of 2.00, indicating the presence of M-OCH₃ initiating group (Table 3, entry 5). The flexibility of the ligand backbone and varied coordination modes of the acetate ligands in 1–4 may also result in multiple active sites during the polymerization process due to change in the molecular symmetry.³⁴ As discussed *vide supra*, complex 1 (Fig. 1) can adopt either a tetrahedral or a trigonal bipyramidal geometry depending on the coordination mode of the acetate ligand.

A more possible route to the formation of low molecular weight and broad molecular weight distributions of PCL obtained is *via* the transesterification reactions.^{30a,32,35} This competes with ring open polymerization to give wide PDI as observed. The concerted low molecular weight and broad PDI confirm the presence of both intramolecular (low molecular weights) and intermolecular (broad PDIs) transesterification reactions. At higher retention times (Fig. S5–S7[†]) broad distributions were observed which could originate from the presence of both cyclic and linear oligomers. In order to confirm

the occurrence of transesterification reactions, ES-MS of the polymers obtained after 4 h and 48 h were recorded (Fig. 9). The polymers showed m/z peaks corresponding to the formula $(n\text{CL} + 17)$ consistent with OH end groups. For example, the m/z peak at 701 corresponds to $\{(114 \times 6) + 17\}$. Significantly, the spectrum of the crude products obtained after 48 h (Fig. 9b) showed smaller peaks corresponding to molecular masses of $\{(n\text{CL} + 1/2\text{CL})\}$ repeat units. As an illustration, the m/z peak at 515 corresponds to $\{(4 \times 114) + 57\}$. This confirms that intermolecular ester-exchange reactions do occur to some extent especially at longer reaction times.³¹ The PDIs of 3.13 and 3.92 reported after 4 h and 48 h respectively reinforces this assumption.

The type of solvent used also affected the polymer weight and molecular weight distribution. A higher molecular weight of 4193 g mol⁻¹ was obtained in reactions performed in toluene compared to 2407 g mol⁻¹ when methanol was used as the solvent (Table 3, entries 5 and 6). This is consistent with the lower rate constant observed when toluene was used as the solvent. As reported in literature, reduced catalytic activities would decrease the number of polymer chains, thus increase molecular weight at a fixed conversion.³⁶ This observations is in good agreement with lower molecular weight of 3119 g mol⁻¹ reported at 90 °C compared to 4610 g mol⁻¹ at 110 °C (Table 3, entries 1 and 7). At higher temperatures, catalyst activity was lower thus decreasing the number of active sites, hence higher molecular weights of the resulted polymers.

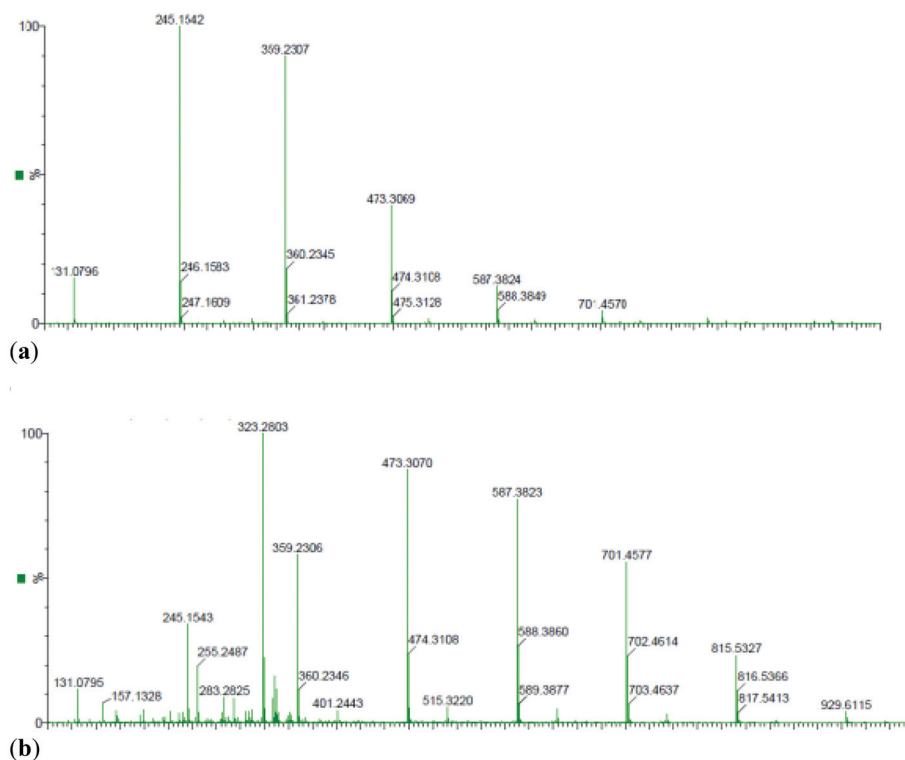


Fig. 9 ES-MS of the crude PCL obtained from (a) catalyst 1; $[\text{CL}]_0/[\mathbf{1}] = 100$, time = 4 h; (b) catalyst 1, $[\text{CL}]_0/[\mathbf{1}] = 100$, time 48 h. The larger peaks corresponds to $(n\text{CL} + 17)$ indicating OH as the end group. The smaller peaks in (b) have masses corresponding to $(n + 1/2\text{CL})$ associated with repeating units from intermolecular transesterification reactions.

Comparatively, initiators **3** and **4** bearing the bulky phenyl groups on the pyrazolyl ring produced relatively higher molecular weight PCL than the corresponding complexes **1** and **2**, containing the less sterically demanding methyl groups (Table 2). For example at 96% conversions, molecular weights of 2928 g mol⁻¹ and 4111 g mol⁻¹ were obtained for **1** and **3** respectively. This could be associated with enhanced chain growth with increase in steric bulk.³⁷ However, there was no significant effect of the identity of the metal on polymer molecular weight. For instance, at 99% conversion, **3** and **4** produced PCL with molecular weights of 4726 g mol⁻¹ and 4652 g mol⁻¹ respectively.

Summary and perspective

In conclusion, we have demonstrated that steric factors control bimetallic or monometallic formation of (pyrazol-1-ylmethyl)pyridine Zn(II) and Cu(II) acetate complexes. The ligands adopt monodentate and bidentate coordination modes in the monometallic and bimetallic complexes respectively. Complexes **1–4** form active and stable catalysts for the ring opening polymerization of ϵ -CL. The kinetics of the polymerization are pseudo-first order in both monomer. Initiator **1** showed first order dependency on the polymerization reactions and utilizes only one of the two possible active sites as the initiating group. The non-rigid nature of the catalyst structure affected the living nature and control of polymer molecular weight of **1–4**. By changing catalyst concentrations, type of solvent and temperature of the reactions, the polymer properties could be regulated. From these results, we believe that through careful ligand design and choice of the initiating group, more efficient catalyst systems with better control of polymer microstructure could be developed.

Experimental section

General materials and methods

All air sensitive manipulations were performed under argon using standard Schlenk line techniques. Compounds 2-(3,5-dimethylpyrazol-1-ylmethyl)pyridine (**L1**) and 2-(3,5-diphenylpyrazol-1-ylmethyl)pyridine (**L2**) were prepared following literature procedures.³⁸ Toluene and hexane solvents were distilled and dried from sodium–benzophenone mixture while dichloromethane was distilled from phosphorous pentoxide. Zn(Ac)₂·2H₂O, Cu(Ac)₂·2H₂O and other chemicals were obtained from Sigma-Aldrich and used as received. The monomer ϵ -CL was purchased from Sigma-Aldrich, vacuum distilled and stored under inert conditions prior to use. NMR spectra were recorded on a Bruker instrument at room temperature in CDCl₃ (¹H at 400 and ¹³C at 100 MHz). Chemical shifts are reported in δ (ppm) and coupling constants are measured in Hertz (Hz). Elemental analyses were recorded on Flash 2000 thermoscientific analyser while mass spectrometry was recorded on a micro-mass LCT premier mass spectrometer.

Electron paramagnetic resonance (EPR) spectra were recorded on a 9.1 GHz Bruker EMX/Premium-240 653 instrument.

[Zn(L1)Ac₂] (1). To a solution of 2-(3,5-dimethylpyrazol-1-ylmethyl)pyridine (**L1**) (0.15 g, 0.80 mmol) in methanol (10 mL) was added a solution of Zn(Ac)₂·2H₂O (0.15 g, 0.80 mmol) in methanol (10 mL) and the solution stirred for 24 h. After the reaction period, the solvent was removed under vacuum to afford a white solid. Recrystallization of the crude product from a dichloromethane–hexane solvent system afforded single-crystals suitable for X-ray analysis. Yield: 0.19 g (63%). ¹H NMR: (400 MHz, CDCl₃): δ , 2.20 (s, 6H, CH₃, Ac); 2.23 (s, 3H, CH₃, pz); 2.54 (s, 3H, CH₃, pz); 5.46 (s, 2H, CH₂); 5.93 (s, 1H, pz); 5.93 (s, 1H, pz); 7.30 (t, 1H, py, ³J_{HH} = 7.2 Hz); 7.43 (d, 1H, py, ³J_{HH} = 7.2 Hz); 7.94 (t, 1H, py, ³J_{HH} = 7.6 Hz); 9.07 (d, 1H, py, ³J_{HH} = 7.6 Hz). ¹³C NMR (CDCl₃): d; 12.13; 14.8; 23.6; 54.1; 108.2; 122.8; 125.1; 138.7; 141.1; 152.3; 153.4; 177.1. ES-MS: *m/z* (%); 309.93 [M⁺ – Ac, 100]; 251.94 [M⁺ – 2Ac, 20]. Anal. Calc. For C₁₅H₁₉N₃O₄Zn: C, 48.60; H, 5.17; N, 11.33. Found: C, 48.31; H, 5.07; N, 11.74.

[Cu(L1)Ac₂] (2). To a solution of **L1** (0.15 g, 0.80 mol) in methanol (10 mL) was added a solution of Cu(Ac)₂·2H₂O (0.16 g, 0.80 mmol) in methanol (10 mL) and the blue solution was stirred for 24 h. Removal of solvent under vacuum gave a deep blue solid material. Recrystallization of the crude product from a dichloromethane–hexane solvent system afforded compound **2** as an analytically pure solid. Yield: 0.19 g (62%). ES-MS: *m/z* (%); 308.93 [M⁺ – Ac, 100]; 249.94 [M⁺ – 2Ac, 20]. Anal. Calc. For C₁₅H₁₉N₃O₄Cu: C, 48.84; H, 5.19; N, 11.39. Found: C, 48.61; H, 5.44; N, 11.18.

[Zn(L2)Ac₂] (3). This compound was prepared according to the procedure describe for **1** using 2-(3,5-diphenylpyrazol-1-ylmethyl)pyridine (**L2**) (0.10 g, 0.32 mmol) and Zn(Ac)₂·2H₂O (0.06 g, 0.32 mmol). Yield: 0.13 g (81%). ¹H NMR: (400 MHz, CDCl₃): δ , 2.20 (s, 6H, CH₃, Ac); 5.59 (s, 2H, CH₂); 6.71 (s, 1H, pz); 5.93 (s, 1H, pz); 7.05 (t, 1H, py, ³J_{HH} = 7.6 Hz); 7.40 (d, 1H, py, ³J_{HH} = 7.2 Hz); 7.44 (m, 4H, ph); 7.86 (m, 2H, ph); 7.64 (m, 4H, ph); 7.70 (t, 1H, py, ³J_{HH} = 7.6 Hz); 8.63 (d, 1H, py, ³J_{HH} = 7.6 Hz). ¹³C NMR (CDCl₃): d; 24.4; 58.2; 109.2; 122.8; 124.1; 125.6; 138.9; 139.1; 142.1; 151.9; 153.8; 178.3. ES-MS: *m/z* (%); 433.88 [M⁺ – Ac, 100]; 373.88 [M⁺ – 2Ac, 20]. Anal. Calc. For C₂₅H₂₃N₃O₄Zn: C, 60.68; H, 4.68; N, 8.49. Found: C, 60.52; H, 4.85; N, 8.78.

[Cu₂(L2)₂Ac₄] (4). This complex was synthesized following the procedure adopted for compound **2** using **L2** (0.10 g, 0.32 mmol) and Cu(Ac)₂·2H₂O (0.06 g, 0.32 mmol). Recrystallization of the crude product from a dichloromethane–hexane mixture afforded single-crystals suitable for X-ray analysis. Yield: 0.10 g (62%). ES-MS *m/z* (%); 308.93 [M⁺ – Ac, 100]; 249.94 [M⁺ – 2Ac, 20]. ES-MS; *m/z* (%); 432.88 [M⁺ – Ac, 100]; 372.88 [M⁺ – 2Ac, 20]. Anal. Calc. For C₅₀H₄₆N₆O₈Cu₂: C, 60.90; H, 4.70; N, 8.52. Found: C, 60.62; H, 4.75; N, 8.67.

X-ray crystallography

Crystal evaluation and data collection of complex **1** and **4** were performed on a Bruker APEXII Duo CCD diffractometer and the reflections were successfully indexed by an automated

indexing routine built in the APEXII program suite.³⁹ A successful solution by the direct methods of SHELXS97 and WinGX32 provided all non-hydrogen atoms from the *E*-map. All non-hydrogen atoms were refined with anisotropic displacement coefficients.⁴⁰ Detailed information are given as ESI.†

General procedure for bulk polymerization of ϵ -caprolactone

Bulk polymerization reactions were performed by introducing an appropriate amount of the complex, depending on the $[\text{CL}]_0/[\text{I}]$ ratio, in a Schlenk tube equipped with a magnetic stirrer under argon. The monomer, ϵ -CL (1.14 g, 0.01 mol) was then added *via* a gas tight syringe and the temperature set at 110 °C before the reactions were initiated. Kinetic experiments were carried out by withdrawing samples at regular intervals (approx. 0.2 mL) using a syringe and quickly quenched by rapid cooling into NMR tubes containing CDCl_3 solvent. The quenched samples were analyzed by ^1H NMR spectroscopy for determination of polymerization of ϵ -CL to PCL. The percentage conversion of $[\text{PCL}]/[\text{CL}]_0 \times 100$, where $[\text{CL}]_0$ is the initial concentration of monomer and $[\text{PCL}]$ is the concentration of the polymer at time t , was evaluated by integration of the peaks for CL (4.2 ppm, OCH_2 signal) and PCL (4.0 ppm, OCH_2 signal) according to the equation $[\text{PCL}]/[\text{CL}]_0 = I_{4.0}/(I_{4.2} + I_{4.0})$ where $I_{4.2}$ is the intensity of the CL monomer signal at 4.2 ppm, and $I_{4.0}$ is the intensity of the PCL signal at 4.0 ppm for the OCH_2 protons. The observed rate constants, K_{obs} , were extracted from the slopes of the lines of best-fit to the plots of $\ln([\text{CL}]_0/[\text{CL}]_t)$ vs. time. The polymers were purified by dissolving the crude products in CH_2Cl_2 followed by addition of cold methanol. A white precipitate was formed, which was isolated by filtration and dried to constant weight prior to analyses by SEC.

Polymer characterization by size exclusion chromatography (SEC)

Polymer samples were dissolved in BHT stabilized THF (2 mg mL^{-1}). The sample solutions were filtered *via* syringe through 0.45 μm nylon filters before analyses. The SEC instrument consists of a Waters 1515 isocratic HPLC pump, a Waters 717plus auto-sampler, Waters 600E system controller (run by Breeze Version 3.30 SPA) and a Waters in-line Degasser AF. A Waters 2414 differential refractometer was used at 30 °C in series with a Waters 2487 dual wavelength absorbance UV/Vis detector operating at variable wavelengths. Tetrahydrofuran (THF, HPLC grade, stabilized with 0.125% BHT) was used as eluent at flow rates of 1 mL min^{-1} . The column oven was kept at 30 °C and the injection volume was 100 μL . Two PLgel (Polymer Laboratories) 5 μm Mixed-C (300 \times 7.5 mm) columns and a pre-column (PLgel 5 μm Guard, 50 \times 7.5 mm) were used. Calibration was done using narrow polystyrene standards ranging from 580 to 2×10^6 g mol^{-1} . All molecular weights were reported as polystyrene equivalents.

Acknowledgements

The authors would like to thank University of KwaZulu-Natal and Third World Academy of Sciences for financial support.

References

- (a) F. Majoumo-Mbe, E. Smolensky, P. Lonneck, D. Shpasser, M. S. Eisen and E. Hey-Hawkins, *J. Mol. Catal. A: Chem.*, 2005, **240**, 91; (b) A. P. Gupta and V. Kumar, *Eur. Polym. J.*, 2007, **43**, 4053; (c) M. Vivas and J. Contreras, *Eur. Polym. J.*, 2003, **39**, 43.
- (a) L. Azor, C. Bailly, L. BreLOT, M. Henry, P. Mobian and S. Dagorne, *Inorg. Chem.*, 2012, **51**, 10876; (b) H. Tian, Z. Tang, X. Zhuang, X. Chen and X. Jing, *Prog. Polym. Sci.*, 2012, **37**, 237; (c) M. G. Davidson, C. T. O'Hara, M. D. Jones, C. G. Keir, M. F. Mahon and G. Kociok-Kohn, *Inorg. Chem.*, 2007, **46**, 7686.
- B. J. O'Keefe, L. E. Breyfogle, M. A. Hillmyer and W. B. Tolman, *J. Am. Chem. Soc.*, 2002, **124**, 4384.
- (a) J. Cayuela, V. Bounor-Legaré, P. Cassagnau and A. Michel, *Macromolecules*, 2006, **39**, 1338; (b) J. Wu, T.-L. Yu, C.-T. Chen and C.-C. Lin, *Coord. Chem. Rev.*, 2006, **250**, 602; (c) B. J. O'Keefe, M. A. Hillmyer and W. B. Tolman, *J. Chem. Soc., Dalton Trans.*, 2001, 2215; (d) K. M. Stridsberg, M. Ryner and A.-C. Albertsson, *Adv. Polym. Sci.*, 2002, **157**, 41.
- (a) H. Du, X. Pang, H. Yu, X. Zhuang, X. Chen, D. Cui, X. Wang and X. Jing, *Macromolecules*, 2007, **40**, 1904; (b) C. Jérôme and P. Lecomte, *Adv. Drug Delivery Rev.*, 2008, **60**, 1056.
- (a) L. E. Breyfogle, C. K. Williams, V. G. Young, M. A. Hillmyer and W. B. Tolman, *Dalton Trans.*, 2006, 928.
- A. C. Albertsson and I. K. Varma, *Adv. Polym. Sci.*, 2002, **157**, 1.
- (a) M. Oshimura, T. Tang and A. Takasu, *J. Polym. Sci., Part A: Polym. Chem.*, 2001, **49**, 1210; (b) Y.-C. Liu, B.-T. Ko and C.-C. Lin, *Macromolecules*, 2001, **34**, 6196.
- (a) D. Thomas, P. Arndt, N. Peulecke, A. Spannenberg, R. Kempe and U. Rosenthal, *Eur. J. Inorg. Chem.*, 1998, 1351; (b) P. Arndt, D. Thomas and U. Rosenthal, *Tetrahedron Lett.*, 1997, **38**, 5467; (c) P. Arndt, A. Spannenberg, W. Baumann and U. Rosenthal, *Eur. J. Inorg. Chem.*, 2001, 2885; (d) A. Asandei and G. Saha, *Macromol. Rapid Commun.*, 2005, **26**, 626; (e) A. Touris, K. Kostakis, S. Mourmouris, V. Kotzabaskis, M. Pitsikalis and N. Hadjichristidis, *Macromolecules*, 2008, **41**, 2426.
- (a) S. K. Russell, C. L. Gamble, K. J. Gibbins, K. C. S. Juhl, W. S. Mitchell, A. J. Tumas and G. E. Hofmeister, *Macromolecules*, 2005, **38**, 10336; (b) Y. Kim and J. G. Verkade, *Macromol. Rapid Commun.*, 2002, **23**, 917; (c) Y. Kim and J. G. Verkade, *Macromol. Symp.*, 2005, **224**, 105; (d) Y. Kim, G. K. Jnaneshwara and J. G. Verkade, *Inorg. Chem.*, 2003, **42**, 1437; (e) Y. Kim and J. G. Verkade, *Organometallics*, 2002, **21**, 2395.
- (a) L. Azor, C. Bailly, L. BreLOT, M. Henry, P. Mobian and S. Dagorne, *Inorg. Chem.*, 2012, **51**, 10876; (b) F. Gornshtein, M. Kapon, M. Botoshansky and M. Eisen, *Organometallics*, 2007, **26**, 497.
- A. J. Chmura, M. G. Davidson, C. J. Frankis, M. D. Jones and M. D. Lunn, *Chem. Commun.*, 2008, 1293.

- 13 (a) C.-Y. Sung, C.-Y. Li, J.-K. Su, T.-Y. Chen, C.-H. Lin and B.-T. Ko, *Dalton Trans.*, 2012, **41**, 953; (b) I. dos Santos Vieira and S. Herres-Pawlis, *Eur. J. Inorg. Chem.*, 2012, 765; (c) T.-P. A. Cao, A. Buchard, X. F. Le Goff, A. Auffrant and C. K. Williams, *Inorg. Chem.*, 2012, **51**, 2157; (d) V. Poirier, T. Roisnel, J.-F. Carpentier and Y. Sarazin, *Dalton Trans.*, 2011, **40**, 523; (e) L. F. Sanchez-Barba, A. Garces, J. Fernandez-Baeza, A. Otero, C. Alonso-Moreno, A. Lara-Sanchez and A. M. Rodriguez, *Organometallics*, 2011, **30**, 2775; (f) R. H. Platel, A. J. P. White and C. K. Williams, *Inorg. Chem.*, 2011, **50**, 7718; (g) J. Wu, Te.-L. Yu, C.-T. Chen and C.-C. Lin, *Coord. Chem. Rev.*, 2006, **250**, 602 and references therein.
- 14 (a) R. R. Gowda and D. J. Chakraborty, *Mol. Catal. A: Chem.*, 2010, **333**, 167; (b) M. Shen, W. Huang, W. Zhang, X. Hao, W.-H. Sun and C. Redshaw, *Dalton Trans.*, 2010, **39**, 9912; (c) A. Arbaoui, C. Redshaw, M. R. J. Elsegood, V. R. Wright, A. Yoshizawa and T. Yamato, *Chem.-Asian J.*, 2010, **5**, 621; (d) N. Nomura, A. Akita, R. Ishii and M. Mizuno, *J. Am. Chem. Soc.*, 2010, **132**, 1750.
- 15 (a) S. O. Ojwach, B. Letitia, I. A. Guzei, J. Darkwa and S. F. Mapolie, *Organometallics*, 2009, **28**, 2127; (b) S. O. Ojwach, I. A. Guzei and J. Darkwa, *J. Organomet. Chem.*, 2009, **694**, 1393.
- 16 G. Parkin, *Chem. Rev.*, 2004, **104**, 699.
- 17 (a) J. Börner, U. Flörke, K. Huber, A. Döring, D. Kuckling and S. Herres-Pawlis, *Chem.-Eur. J.*, 2009, **15**, 2362; (b) S. O. Ojwach, G. S. Nyamato, B. Omondi, J. Darkwa and A. O. Okoth, *J. Coord. Chem.*, 2012, **65**, 298.
- 18 F. A. Allen, *Acta Crystallogr.*, 2002, **B58**, 380.
- 19 (a) M. Casarin, C. Corvaja, C. D. Nicola, D. Falcomer, L. Franco, M. Monari, L. Pandolfo, C. Pettinari and F. Piccinelli, *Inorg. Chem.*, 2005, **44**, 6265; (b) N. Judas, *Acta Crystallogr., Sect. E: Struct. Rep. Online*, 2005, **61**, 2217.
- 20 (a) C. Harding, V. McKee and J. Nelson, *J. Am. Chem. Soc.*, 1991, **113**, 9684; (b) J. Casanova, G. Alzuet, J. Latorre and J. Borra's, *Inorg. Chem.*, 1997, **36**, 2052; (c) R. Sarma, A. K. Boudalis and J. B. Baruah, *Inorg. Chim. Acta*, 2010, **363**, 2279.
- 21 (a) S. J. Brown, X. Tao, D. W. Stephan and P. K. Mascharak, *Inorg. Chem.*, 1986, **25**, 3377; (b) C. P. Pradeep, P. S. Zacharias and S. K. Das, *J. Chem. Sci.*, 2005, **117**, 133; (c) A. Ozarowski, I. B. Szymanska, T. Muziol and J. Jezierska, *J. Am. Chem. Soc.*, 2009, **131**, 10279; (d) A. Ozarowski, *Inorg. Chem.*, 2008, **47**, 9760.
- 22 D. L. Reger, A. Debreczeni and M. D. Smith, *Inorg. Chem.*, 2012, **51**, 1068.
- 23 S. J. Brown, X. Tao, T. A. Wark, D. W. Stephan and P. K. Mascharak, *Inorg. Chem.*, 1988, **27**, 1581.
- 24 G. F. Kokoszka, M. Linzer and G. Gordon, *Inorg. Chem.*, 1968, **7**, 1730.
- 25 M. Labet and W. Thielemans, *Chem. Soc. Rev.*, 2009, **38**, 3484.
- 26 C. M. Silvernail, L. Y. Yao, L. M. R. Hill, M. A. Hillmyer and W. B. Tolman, *Inorg. Chem.*, 2007, **46**, 6565.
- 27 (a) C. K. Williams, L. E. Breyfogle, S. Kyung Choi, W. Nam, V. G. Young Jr., M. A. Hillmyer and W. B. Tolman, *J. Am. Chem. Soc.*, 2003, **125**, 11350; (b) H.-Y. Chen, B.-H. Huang and C.-C. Lin, *Macromolecule*, 2005, **38**, 5400.
- 28 Z. Zhong, P. J. Dijkstra and J. Feijen, *J. Am. Chem. Soc.*, 2003, **125**, 11298.
- 29 A. Kowalski, J. Libsiszowski and S. Penczce, *Macromolecules*, 2001, **33**, 1964.
- 30 (a) P. Dubois, C. Jacobs, R. Jerome and P. Teyssie, *Macromolecules*, 1991, **24**, 2266; (b) T. Ouhadi, C. Stevens and P. Teyssie, *Makromol. Chem., Suppl.*, 1975, **1**, 191; (c) V. J. Shiner, D. Whittaker and V. P. Fernandez, *J. Am. Chem. Soc.*, 1963, **85**, 2318.
- 31 C. K. Williams, L. E. Breyfogle, S. K. Cho, W. Nam, V. G. Young, M. A. Hillmyer and W. B. Tolman, *J. Am. Chem. Soc.*, 2003, **125**, 11350.
- 32 (a) W. M. Stevels, M. J. Ankone, P. J. Dijkstra and J. Feijen, *Macromolecules*, 1996, **29**, 6132; (b) B. M. Chamberlain, B. A. Jazdzewski, M. Pink, M. A. Hillmyer and W. B. Tolman, *Macromolecules*, 2000, **33**, 3970; (c) S. J. McClain, T. M. Ford and N. E. Drysdale, *Polym. Prepr. (Am. Chem. Soc., Div. Polym. Chem.)*, 1992, **33**, 463.
- 33 B. M. Chamberlain, B. A. Jazdzewski, M. Cheng, D. R. Moore, T. M. Ovitt, E. B. Lobkovsky and G. W. Coates, *J. Am. Chem. Soc.*, 2001, **123**, 3229.
- 34 (a) P. J. Shapiro, W. P. Schaefer, J. A. Labinger and J. E. Bercaw, *J. Am. Chem. Soc.*, 1994, **116**, 4623; (b) R. M. C. Waymouth, *Science*, 1995, **267**, 217.
- 35 (a) H. R. Kricheldorf, J. M. Jonte and M. Berl, *Makromol. Chem., Suppl.*, 1985, **12**, 25; (b) H. R. Kricheldorf, T. Mang and J. M. Jonte, *Macromolecules*, 1984, **17**, 2174.
- 36 (a) T. M. Ovitt and G. W. Coates, *J. Polym. Sci., Part A: Polym. Chem.*, 2000, **38**, 4686; (b) G. Odian, *Principles of Polymerization*, John Wiley & Sons, New York, 1991, pp. 535–540.
- 37 (a) D. J. B. Temple, *Organometallics*, 1998, **17**, 2290; (b) S. A. Svejda, L. K. Jonhson and M. Brookhart, *J. Am. Chem. Soc.*, 1999, **121**, 10634.
- 38 (a) P. J. Steel, A. A. Watson and D. A. House, *Inorg. Chim. Acta*, 1987, **130**, 167; (b) S. O. Ojwach, I. A. Guzei, J. Darkwa and S. F. Mapolie, *Polyhedron*, 2007, **26**, 851.
- 39 Bruker-AXS, Madison, Wisconsin, USA, 2009.
- 40 (a) G. M. Sheldrick, *Acta Crystallogr.*, 2008, **A64**, 112; (b) *SADABS Area-Detector Absorption Correction*, Siemens Industrial Automation, Inc., Madison, WI, 1996; (c) *SAINT Area-Detector Integration Software*, Siemens Industrial Automation, Inc., Madison, WI, 1995.